Proceedings of the ASME 2022 17th International Manufacturing Science and Engineering Conference **MSEC2022**

June 27-July 1, 2022, West Lafayette, Indiana, USA

MSEC2022-85383

OPTIMIZATION-BASED DISASSEMBLY SEQUENCE PLANNING UNDER **UNCERTAINTY FOR HUMAN-ROBOT COLLABORATION**

Hao-yu Liao

Graduate Research Assistant **Environmental Engineering Sciences** University of Florida, Gainesville, FL, 32611 haoyuliao@ufl.edu

Boyi Hu

Assistant Professor Industrial and Systems Engineering University of Florida, Gainesville, FL, 32611 bovihu@ise.ufl.edu

ABSTRACT

Disassembly is an integral part of maintenance, upgrade, and remanufacturing operations to recover end-of-use products. Optimization of disassembly sequences and the capability of robotic technology are crucial for managing the resourceintensive nature of dismantling operations. This study proposes an optimization framework for disassembly sequence planning under uncertainty considering human-robot collaboration. The proposed model combines three attributes: disassembly cost, disassembleability, and safety, to find the optimal path for dismantling a product and assigning each disassembly operation among humans and robots. The multi-attribute utility function has been employed to address uncertainty and make a tradeoff among multiple attributes. The disassembly time reflects the cost of disassembly and is assumed to be an uncertain parameter with a Beta probability density function; the disassembleability evaluates the feasibility of conducting operations by robot; finally, the safety index ensures the safety of human workers in the work environment. The optimization model identifies the best disassembly sequence and makes tradeoffs among multiattributes. An example of a computer desktop illustrates how the proposed model works. The model identifies the optimal disassembly sequence with less disassembly cost, high disassembleability, and increased safety index while allocating disassembly operations between human and robot. A sensitivity analysis is conducted to show the model's performance when changing the disassembly cost for the robot.

Keywords: Human-robot collaboration, Disassembly sequence planning, Optimization, Uncertainty, Remanufacturing

Yuhao Chen

Graduate Research Assistant Industrial and Systems Engineering University of Florida, Gainesville, FL, 32611 yuhaochen@ufl.edu

Sara Behdad*

Associate Professor **Environmental Engineering Sciences** University of Florida, Gainesville, FL, 32611 sarabehdad@ufl.edu

NOMENCLA	ATURE
U(y)	The utility function of variable <i>y</i>
f(y)	The probability density function of attribute <i>y</i>
f(t)	The probability distribution of disassembly
	time
Γ	Gamma function
p,q	Shape parameters of the beta distribution
$C_i(t)$	Disassembly cost of task j
d, c	Constant parameters of the disassembly cost
	function
U_{i}	The overall utility of task j
DS	Disassembleability scores
SI	Strain index scores
t_U , t_L	Upper and lower bounds for disassembly
	time
t	disassembly time
C_{max}	Maximum disassembly cost
C_{min}	Minimum disassembly cost
SI_{max}	Maximum strain index
SI_{max}	Minimum strain index
DS_{max}	Maximum disassembleability score
DS_{min}	Minimum disassembleability score
	WATER W

1. INTRODUCTION

Proper recovery of electronic waste (e-waste) has considerable environmental and economic benefits [1]. Various financial and social strategies have been suggested for managing the e-waste problem [2][3]. One approach to reducing e-waste is extending the product life cycle through reuse, remanufacture, or recovery of components [4]. Disassembly is an unavoidable step for the proper recovery of components. One question often facing remanufacturers is identifying the best way to dismantle a device or find the optimal disassembly sequences [5].

The optimal disassembly sequence provides cost-effective solutions to reduce the resource-intensive nature of recovery operations. Disassembly is an essential step for most recovery operations such as remanufacturing [6], maintenance [7], upgrade [8], and recycling [9]. Various normative models have been developed to find the optimal disassembly sequence. To name a few studies, Tseng et al. (2020) used the flatworm algorithm to lower disassembly times by reducing the amount of disassembly direction and required tools [10]. Fu et al. (2021) proposed a stochastic bi-objective disassembly planning to maximize profit while minimizing energy consumption [11]. Xia et al. (2020) developed a 3D-based multi-objective collaborative disassembly sequence planning method by prioritizing disassembly levels for parts [12]. Lee et al. (2020) applied a fuzzy scoring procedure to measure disassembly factors before using a genetic algorithm to select the best sequence [13]. Behdad and Thurston used multi-attribute utility theory to determine the optimal disassembly sequence considering multiple attributes of cost and probability of components damage during disassembly and reassembly [7], [14]. While the previous studies have investigated disassembly sequence planning, the number of studies considering robotic-assisted disassembly and human-robot collaboration is limited.

Human-robot collaboration in disassembly is becoming a popular topic in recent years. Disassembly tasks' labor-intensive and repetitive nature may lead to human musculoskeletal disorders [15]. Robots can handle monotonous repetitive or hazardous tasks more efficiently than humans [15], [16]. Although robots provide higher efficiency, human workers are still needed in disassembly operations for handling tasks that are difficult and inflexible for robots [17].

considered Previous studies have collaboration when deciding on disassembly sequence planning. For example, Lee et al. (2020) considered disassembly rules, disassembly cost, and the position between human worker and robot and used a receding horizon control technique for real-time disassembly planning [18]. Xu et al. (2020) applied a discrete bees algorithm to determine disassembly sequence planning by considering time, cost, and difficulty of disassembly [17]. Parsa and Saadat (2021) used a genetic algorithm to optimize sequence planning, considering cleanability, repairability, and economy [19]. Xu et al. (2019) adopted a multi-objective artificial bee colony algorithm and AND/OR graph to find the optimal disassembly sequence considering disassembly failure risks, disassembly priority, cycle time, and cost [20]. Li et al. (2019) considered human fatigue to evaluate disassembly efficiency and used the bees algorithm to arrange tasks among humans and robots [15]. Xu et al. (2021) considered the safety strategy and disassembly time and used the improved discrete bees algorithm to allocate disassembly tasks [21]. Their safety strategy is to

consider the location between human workers and robots. As a human worker approaches the robot, the operation speed of the robot will slow down to avoid robot accidents.

Although previous researchers considered different factors when allocating tasks in human-robot collaboration, no study has considered disassembly cost, disassembleability, and safety to the best of our knowledge. Combining additional attributes and considering the uncertainty are the primary contributions of this study. We propose a new optimization-based disassembly sequence planning by considering multiple attributes, including disassembly cost, disassembleability, and safety. The study uses a multi-attribute utility function to combine these different attributes. Moreover, it considers the disassembly time as an uncertain variable with a Beta probability distribution [22]. Besides disassembly cost (time), we also consider disassembly [19], [23], and the operator safety, which is modeled by using the strain index [24].

The objective of the study is to find the optimal disassembly sequence and allocate tasks between humans and robots. The feasible disassembly sequences for a given product can be presented in the form of a graph, as shown in Figure 1, for a simple product with three components. Each path has different costs, safety, and difficulty.

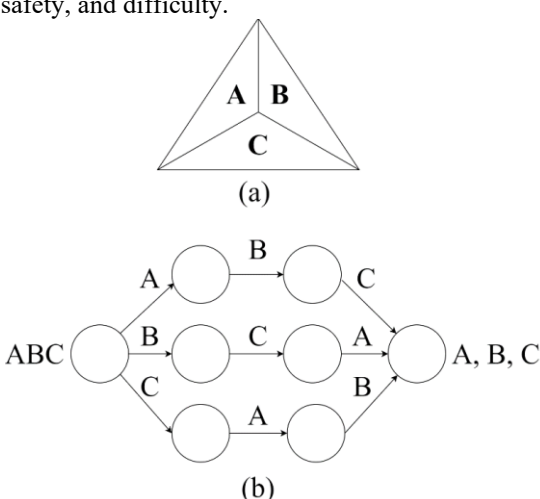


Figure 1: A simple product with three components (a) and feasible disassembly sequences (b).

2. METHODOLOGY

This section describes different attributes that have been considered in the objective function and the proposed optimization model. The concept of a multi-attribute utility function is used to integrate the three attributes.

2.1 Utility function

The three objectives considered in this study include disassembly cost, disassembleability, and safety. The individual utility functions of these three attributes have been integrated to form the overall utility function as shown in Eqs. (1)-(3). $U_{a,j}$ shows the utility function of attribute a for disassembly task j, and k_a is the scaling constant for attribute a. The scaling

constant K is determined using Eq. (2). The implementation details can be found in Refs [25]–[27].

$$U_{j} = \sum_{i \in I} \frac{1}{K} \left\{ \prod_{a \in A} [Kk_{a}U_{a,j} + 1] - 1 \right\}$$
 (1)

$$1 + K = \prod_{a \in A} [Kk_a + 1] \tag{2}$$

$$U_{a,j} = E[U(y)] = \int U(y)f(y)dy$$
 (3)

The scaling constant K is found through Eq. (2). Since some attributes such as disassembly time are uncertain, we have used the expected utility instead of utility function U(y). If the attribute is uncertain with the probability density function f(y)The utility function will be calculated by Eq. (3) to use the expected value. For details, see [25]–[27].

In addition, each attribute is normalized by min-max normalization since the unit and range of each attribute are different. Also, each attribute is utility independent of other attributes. According to Clemen and Reilly, an attribute is utility independent of another attribute, if preferences for uncertain choices possessing different attribute levels are independent of the values of another attribute [28]. For example, disassembly cost and disassembleability are preferentially independent and utility independent since, regardless of the value of disassembly cost, the user always prefers lower complexity (higher disassembleability) over higher complexity. Even in the case of different uncertain choices involving values disassembleability, the user's preference among the uncertain cases is independent of disassembly cost. We should note that the concept of preferential independence and utility independence is separate from how attributes are calculated.

2.2 Disassembly cost

The disassembly cost depends on the disassembly time which is modeled as an uncertain variable. Fischer et al. (2005) showed that the disassembly time could be well described as a Beta distribution [22]:

$$\begin{cases} f(t) = \frac{\Gamma(p+q)}{r\Gamma(p)\Gamma(q)} \left(\frac{t-t_L}{r}\right)^{p-1} \left(\frac{t_U-t}{r}\right)^{q-1} & \text{if } t_L \le t \le t_U \\ = 0 & \text{Othetwise} \end{cases}$$
(4)

where
$$r = t_U - t_L$$
 (5)

The t_U and t_L is the range of disassembly time, p,q are shape parameters, and Γ is the gamma function.

This study assumes that the cost and time have an exponential function, as expressed in Eq. (6) since the higher time results in more human fatigue, lower performance, and higher opportunity costs. Glock et al. used exponential function to describe human fatigue [29], and Potkonjak et al. introduced robot fatigue and mentioned that fatigue quantification is often assumed to be exponential [30].

$$C_i(t) = de^{ct} (6)$$

where $C_j(t)$ is the disassembly cost of task j with disassembly time t, and d, and c are the constant parameters. The utility function for disassembly cost has been considered as follows:

$$U(C_j) = \frac{c_j(t) - c_{min}}{c_{max} - c_{min}} \tag{7}$$

where
$$C_{max} = de^{ct_{max}}$$
 and $C_{min} = de^{ct_{min}}$ (8)

The utility function of cost is normalized between 0 and 1. C_{max} and C_{min} are the maximum and minimum disassembly costs. Given the uncertain disassembly time, the expected disassembly cost is described as:

$$E[U(C_j)] = \int_{t_L}^{t_U} \left(\frac{C_j(t) - C_{min}}{C_{max} - C_{min}}\right) f(t) dt$$

$$= g \int_{t_L}^{t_U} \left(\frac{C_j(t) - C_{min}}{C_{max} - C_{min}}\right) \left(\frac{t - t_L}{r}\right)^{p-1} \left(\frac{t_U - t}{r}\right)^{q-1} dt$$
(9)

where
$$g = \frac{\Gamma(p+q)}{r\Gamma(p)(q)}$$
 (10)

2.3 Operator safety

Besides disassembly cost, operator safety is another important attribute. The Strain Index (SI), proposed by Moore and Garg in 1995 [24], is a well-known tool to evaluate the risk of developing musculoskeletal disorders in distal upper extremities, including the hand, wrist, forearm, and elbow. Given that the e-waste disassembly task requires a lot of upper limb movements, such as disconnecting cables and loosening screws, the SI score is a suitable method to quantify human physical stress in our study. The disassembly tasks are assigned to human and robot based on SI scores to release human physical stress.

The SI score is determined based on the subjective ratings of six task variables, including 1) intensity of exertion (IE), 2) duration of exertion (DE), 3) efforts per minute (EM), 4) hand/wrist posture (HWP), 5) speed of work (SW), and 6) duration per day (DD). A multiplier is then assigned to each task variable based on the ratings. Based on Moore and Garg [24], the rating criteria of the six task variables and their corresponding multipliers are summarized in Tables 1 and 2, respectively. Finally, the SI score is computed by taking the product of the six multipliers:

$$SI = IE' \times DE' \times EM' \times HWP' \times SW' \times DD'$$
 (11)

Table 1: The rating criterion of the six SI task variables [24].

Rating	IE	DE	EM	HWP	SW	DD
1	Light	< 10	< 4	Very good	Very slow	≤ 1
2	Somewhat hard	10-29	4-8	Good	Slow	1-2
3	Hard	30-49	9-14	Fair	Fair	2-4
4	Very Hard	50-79	15-19	Bad	Fast	4-8
5	Near	> 80	≥ 20	Very	Very	> 8
<i></i>	Maximal	≥ 80	≥ 20	bad	fast	- 0

Table 2: The multipliers of the six SI task variables [24].

Rating	IE'	DE'	EM'	HWP'	SW'	DD'
1	1	0.5	0.5	1.0	1.0	0.25
2	3	1.0	1.0	1.0	1.0	0.50
3	6	1.5	1.5	1.5	1.0	0.75
4	9	2.0	2.0	2.0	1.5	1.00
5	13	3.0	3.0	3.0	2.0	1.50

2.4 Disassembleability

The third attribute considered for determining optimal sequence is disassembleability. The disassembleability describes the level of complexity of each disassembly task. Tasks with lower disassembleability are not feasible for the robot. The parameters describing disassembleability are introduced in [19], [23] which include: 1) component size (CS), 2) component weight (CW), 3) requirement of tools (T), 4) accessibility (AC), 5) component shape (CSH), 6) operation complexity (OC), 7) positioning (P), and 8) operation force (OF). The scores of each parameter are described in Table 3.

Table	Table 3: The eight disassembleability parameters [19], [23].					
CS	Easily grasped	2				
	Moderately difficult to grasp	3.5				
	Difficult to grasp	4				
\mathbf{CW}	Light	2				
	Moderately heavy	2.2				
	Very heavy	2.4				
T	No tools required	1				
	Common tools required	2				
	Specialized tools required	3				
\mathbf{AC}	Shallow and broad fastener recesses	1				
	Deep and narrow fastener recesses	1.6				
	Very deep and very narrow fastener recesses	2				
CSH	Symmetric	0.8				
	Semi-symmetric	1.2				
	Asymmetric	1.4				
\mathbf{OC}	Low	1				
	Moderate	4.5				
	High	6.5				
P	No accuracy required	1.2				
	Some accuracy required	2				
	High accuracy required	5				
OF	Low	1				
	Moderate	2				
	High	4				

The disassembleability score (DS) is computed by summing up the eight parameters:

$$DS = CS + CW + T + AC + CSH + OC + P + OF$$
 (12)

According to [19], [23], if DS is higher than 14.2 or the robot's capability, the tasks are assigned to the human worker since they exceed the robot's capability. For example, if the object is too small or too heavy, the robot cannot hold and locate the position; therefore, those tasks are assigned to the human worker.

2.5 The optimization-based disassembly sequence planning framework for human-robot collaboration

The multi-attribute utility function U_i shows the overall utility of disassembly operation j, which incorporates the three individual utility functions of disassembly disassembleability, and safety. U_i will be used to formulate the objective function of the optimization model. The objective is to maximize the overall utility of the whole sequence. A binary decision variable x_i is defined to determine whether disassembly operation j should be conducted or not. The safety SI scores are used to assign each task to the human worker or robot. Due to the high complexity and uncertainty, the tasks with high DS values are given to the human worker. The index set, decision variable, and model parameters are expressed as follows:

Index	set
-------	-----

j	Feasible disassembly transition j (task)
J	The set of all feasible disassembly transitions
a	Attribute a
S	The set of all attributes
M_n	The set of all disassembly transitions going to node <i>n</i>
O_n	The set of all disassembly transitions outgoing from node n
I	The set of all feasible initial disassembly transitions
F	The set of all feasible finial disassembly transitions

Decision Variables

x_i	Binary variable $\{0, 1\} = \{\text{not performed}, \}$
,	performed) whether disassembly transition j is
	performed.
α_i	Binary variable $\{0, 1\} = \{\text{performed by robot}, \}$
,	performed by human} whether disassembly
	transition <i>i</i> is performed by robot or human.

Parameters

$U_{a,j}$	The single utility function of attribute <i>a</i> for
	transition j
$E[U(C_{R,j})]$	The expected disassembly cost of a robot
$E[U(C_{H,i})]$	The expected disassembly cost of human
. ,,,	workers
k_a	The scaling constant (a value between 0 to 1)
K	The overall scaling constant (between 0 to 1)
ST, DT	The threshold of SI scores and DS
Μ	A large enough number. Ex. 10^{10}
y_j	Binary variable {0, 1}

The proposed optimization model for disassembly sequence planning is expressed as:

$$Max \sum_{j \in J} \frac{1}{K} \left\{ \prod_{a \in S} \left[K k_a U_{a,j} + 1 \right] - 1 \right\} x_j$$
 (13)

Subject to:

$$U_{1,j} = (1 - \alpha_j) E[U(C_{R,j})] + \alpha_j E[U(C_{H,j})]$$
 (14)

$$U_{2,j} = \frac{SI_{max} - SI_j}{SI_{max} - SI_{min}} \tag{15}$$

$$U_{3,j} = \frac{DS_{max} - DS_{j}}{DS_{max} - DS_{min}}$$
 (16)

$$(1-\alpha_i) \cdot (DT - DS_i) \ge 0 \tag{17}$$

$$M(1 - y_i) \ge (DT - DS_i) \tag{18}$$

$$\alpha_i(ST - SI_i) + M \cdot y_i \ge 0 \tag{19}$$

$$\sum_{i \in I} x_i = 1 \text{ (initial node)}$$
 (20)

$$\sum_{j \in M_n} x_j = \sum_{j \in O_n} x_j \text{ (transit nodes)}$$
 (21)

$$\sum_{i \in F} x_i = 1 \text{ (target node)}$$
 (22)

$$U_{\alpha,j} \in \left\{ U_{1,j} \; , \; U_{2,j} \; , \; U_{3,j} \right\} \tag{23}$$

$$0 \le U_{a,j} \le 1 \quad \forall a, \forall j \tag{24}$$

Eq. (14) shows the expected disassembly cost of the human worker and robot can be derived from Eq. (9). Eqs. (15) and (16) reflect each task's SI scores and DS normalizing between 0 and 1. Eq. (17) to (19) is a set of inequalities representing an if-then statement when solving the task assignment between human and robot. When the task has high safety and high disassembleability, it can be assigned to either robot or human; if the expected disassembly cost of the robot is less than the expected disassembly cost of the human worker, the α_j will be 0. In addition, the SI scores and DS also determine the α_j based on the condition of safety and disassembleability.

3. CASE STUDY

The study uses data collected from the disassembly of a Dell desktop computer as a case study.

Three main components are targeted for disassembly (as shown in Figure 2a), i.e., component A - heatsink assembly, component B - optical disc drive & hard drive assembly, and component C - memory module. The heatsink assembly, as illustrated in Figure 2b, is made up of a fan shroud (A1) and a heat sink (A2), whereas component B consists of an optical disc drive (B1) and a hard drive (B2).

The number of possible disassembly sequences of the three components could be understood as a permutation problem, i.e., there are six permutations of the set {A, B, C}, namely (A, B, C), (A, C, B), (B, A, C), (B, C, A), (C, A, B), and (C, B, A).



Figure 2: The desktop components targeted for disassembly.

All six possible sequences are verified to be feasible in our pilot tests. However, the removal of sub-assemblies had to be in specific orders due to physical constraints. Specifically, to remove the heatsink assembly (A) from the computer, the fan shroud (A1) had to be removed before the heat sink (A2) so that the cable of A2 could be disconnected from the system board. Similarly, to remove component B from the computer, one had to remove the optical disc drive (B1) first to get access to the hard drive (B2). Figure 4 shows the possible disassemble sequences.

To evaluate the SI and DS scores, a participant was tasked with removing the heatsink assembly, the optical disc drive, the hard drive, and the memory module from the desktop computer. Adequate training was given to the participant before the formal data collection. The manufacturer's service manual guided the disassembly procedure. The participant was videotaped during the data collection, performing the disassembly task. After the task was accomplished, the participant was interviewed about their subjective rating of force-related variables, i.e., IE of SI and OF of DI, for every work element. The disassembly of each component is composed of different tasks as shown in Table 4.

Two researchers independently analyzed the video taken during the data collection to obtain the remaining variables. Instead of computing the SI score for the entire job, SI scores for every work task were calculated in the study to validate our optimization model. Furthermore, a default rating value of 4 was assigned to DD, representing a worker performing a given task for 4–8 h [31].

Table 5 shows the disassembly time for human and robot. In this example, the lower bound of disassembly time, t_L for human is determined from experiments. The upper bound of disassembly time for human, t_U , and disassembly times of robot are assumed.

The disassembly time by the robot is assumed to be greater than human due to the current software and hardware limitations of the robots in handling disassembly tasks. The robotic technology for disassembly tasks is not well developed, and most disassembly operations are still conducted manually, so we assume a higher operation time for robots to handle tasks. This may change in the future with more advancements in robotics.

Table 4: The disassembly tasks of each component.

Component	Task	Action			
	J1	Push away the two release handles while lifting the fan shroud upward and off the computer			
Remove Heatsink Assembly (A) (For paths	J2	Disconnect the fan cable (with clip) from the system board.			
1 to 6)	J3	posen the captive screws (x4).			
	J4	ift the heat sink assembly and remove it from the computer.			
	J5	Disconnect the data cable from the back of the optical drive.			
	J6	Disconnect the power cable from the back of the optical drive.			
Remove Optical Disc Drive & Hard Drive	J7	Lift the tab and slide the optical drive out.			
Assembly (B) (For paths 1 to 6)	J8	Disconnect the data cable from the back of the optical drive.			
Assembly (B) (For paths 1 to 0)	J9	Disconnect the power cable from the back of the optical drive.			
	J10	Slide the blue drive-cage handle toward the unlocking position.			
	J11	Lift the hard drive cage from the computer.			
Remove RAM (C) (For paths 1 & 2,	J12	Press down on the memory retaining tabs on each side of the memory module.			
Remove C after removing A and B)	J13	Lift the memory module out of the connectors on the system board.			
Remove RAM (C) (For paths 3 & 4,	J14	Press down on the memory retaining tabs on each side of the memory module.			
Remove C between A and B)	J15	Lift the memory module out of the connectors on the system board.			
Remove RAM (C) (For paths 5 & 6, J16 Press down on the memory retaining tabs on each side of the memory module.		Press down on the memory retaining tabs on each side of the memory module.			
Remove C before removing A and B)	J17	Lift the memory module out of the connectors on the system board.			

Table 5: The disassembly time by human and robot.

Task	Huma	n worker	Robot	Robot	
Task	t_L	t_U	t_L	t_U	
J1	3	8	4	9	
J2	3	8	11	16	
J3	53	58	87	92	
J4	2	7	3	8	
J5	3	8	11	16	
J6	3	8	11	16	
J7	3	8	4	9	
Ј8	3	8	15	20	
Ј9	3	8	15	20	
J10	2	7	3	8	
J11	4	9	5	10	
J12	3	8	8	13	
J13	2	7	3	8	
J14	3	8	9	14	
J15	2	7	3	8	
J16	4	9	16	21	
J17	2	7	6	11	

Table 6 summarizes the SI scores and DS for each task. While the component A removal and component B removal of SI scores and DS are the same in each possible disassembly sequence planning, the disassembly of component C was highly dependent on the disassembly order of component A removal and component B removal.

As shown in Figure 2a, if component C is removed before B and A, the limited space could negatively impact variables such as HWP of SI scores and AC and P of DS. Moreover, poor hand/wrist posture and accessibility made the force exertion more difficult, increasing the subjective ratings of IE of SI and of DS. Consequently, the SI scores and DS are higher when component C was removed before A and B, performing tasks J16 and J17, and they dropped if A or B was removed before C, performing tasks J12 and J13.

Table 6: The results of SI scores and DS for each task.

Task	SI scores	DS	Task	SI scores	DS
J1	9	11.2	J10	9	12
J2	18	16.3	J11	18	12
J3	13.5	19.8	J12	9	15.3
J4	9	10	J13	9	10.8
J5	40.5	16.3	J14	13.5	15.9
J6	40.5	16.3	J15	13.5	11.4
J7	9	10.8	J16	54	17.3
Ј8	54	17.3	J17	18	14.8
J9	54	17.3			

Regarding input parameters, the parameter d in disassembly cost for human and robot is assumed to be 5 and 2, respectively, and parameter c is 0.01 in Eq. (6). Due to this study's limited time and scope, we run each disassembly operation only once; however, one experiment is not enough to obtain the exact shape of the distribution function. In practice, comprehensive data collection is needed to experimentally gather disassembly time, fit the proper distribution, and estimate the parameters of the distribution functions. The relation between disassembly cost and time is plotted in Figure 3.

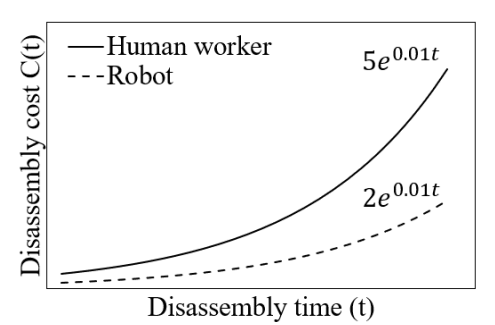


Figure 3: The disassembly cost of human and robot.

The robot costs less than the human worker due to its capability in handling long-term monotonous, repetitive tasks [15], [16]. Also, the scaling constants K, k_1 , k_2 , and k_3 are considered as 1.68, 0.17, 0.3, 0.23. According to Table 6, the tasks with SI scores higher than 18 are assigned to the robot to reduce musculoskeletal disorders damage to the human worker.

4. RESULTS AND DISCUSSIONS

This section shows the results of the work assignments between human and robot for the case of disassembling a Dell desktop computer. In addition, several sensitivity analyses on parameters (d and c) of the cost function have been conducted.

4.1 The Optimal disassembly sequence for the desktop components

The utility of each attribute and the task assignment among human and robot is shown in Table 7. Some utilities are 0 due to normalization. These tasks reflect either a high SI or high DS score. For example, $U_{3,i}$ of task J3 equals 0, meaning this task has high values of DS that the robot cannot implement. The action of J3 is to loosen the captive four screws. This task needs high positioning with these small object screws with high complexity and uncertainty. Thus, the task is assigned to the human worker. Some tasks are decided by expected cost when the tasks have low SI scores and high disassembleability. For example, task J4 is to lift the heat sink assembly and remove it from the computer with low SI scores and low DS. The task is assigned to the robot due to cost-efficiency. Although the robot's disassembly time is higher than that of human workers, the expected disassembly cost of the robot is less than the expected disassembly cost of humans, as previously discussed in Figure 3. However, tasks with high SI and DS scores, for example, J9, are assigned to the human worker. Although task J9 has a safety

issue, it is still assigned to humans due to the high operational complexity and infeasibility.

Table 7: The results of multi-attribute utilities and overall utility for each task (R: robot; H: human worker).

Task	$U_{1,j}$	$U_{2,j}$	$U_{3,j}$	Overall Utility U_j	Work Assign
J1	0.98	1.00	0.88	0.94	R
J2	0.97	0.80	0.36	0.62	Н
J3	0.08	0.90	0.00	0.29	Н
J4	0.99	1.00	1.00	1.00	R
J5	0.97	0.30	0.36	0.40	H
J6	0.97	0.30	0.36	0.40	Н
J7	0.98	1.00	0.92	0.96	R
Ј8	0.97	0.00	0.26	0.24	H
J9	0.97	0.00	0.26	0.24	Н
J10	0.99	1.00	0.80	0.90	R
J11	0.97	0.80	0.80	0.80	R
J12	0.97	1.00	0.46	0.75	Н
J13	0.99	1.00	0.92	0.96	R
J14	0.97	0.90	0.40	0.68	Н
J15	0.99	0.90	0.86	0.88	R
J16	0.95	0.00	0.26	0.24	Н
J17	0.98	0.80	0.51	0.68	Н

Figure 5 shows the optimal sequence. Paths 1-2-8-14 and 1-3-9-14 have the same overall utilities, 8.49, so either path is optimum. The difference between them is that path 1-2-8-14 removes component A before B, and path 1-3-9-14 removes B before A. Paths 1-4-10-14 and 1-5-11-14 have the same utility, 8.34. Both paths remove component C after A or B. Paths 1-6-12-14 and 1-7-13-14 have the lowest utility of 7.70 since component C is removed first in both paths with limited space.

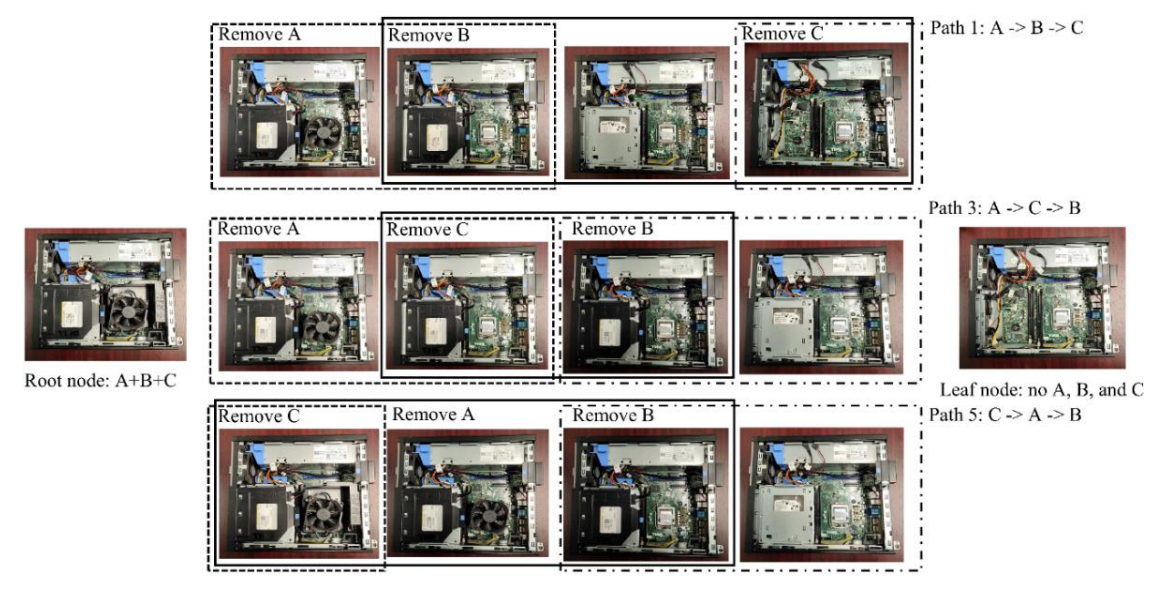


Figure 4: The three possible disassemble sequences for components A (heatsink assembly), B (optical disc drive & hard drive assembly), and C (memory module)

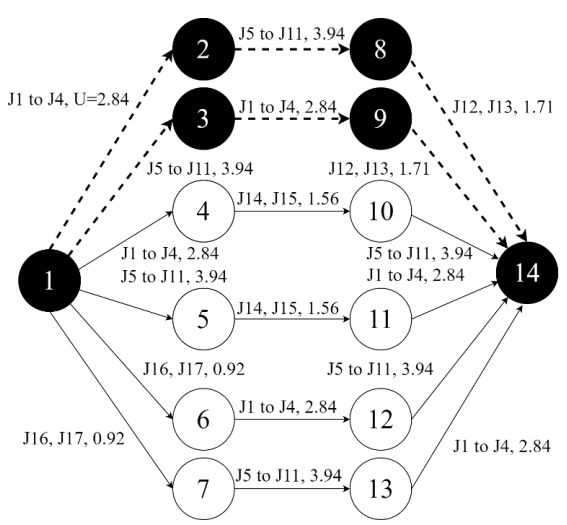
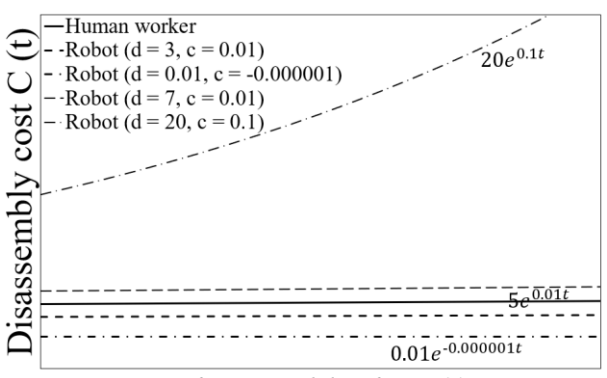


Figure 5: The summary of feasible and optimal disassembly paths.

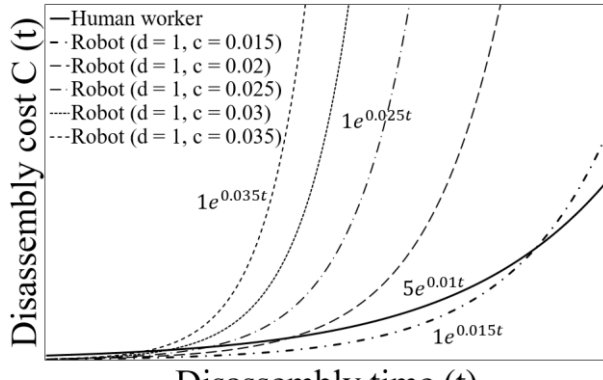
4.2 Sensitivity analysis of the cost function

Three different conditions of the cost function are discussed by considering different combinations of parameters d and c. The cost function of the human worker is the same as in the previous section, with parameters d=5 and c=0.01. Figures 6 to 8 show the three different conditions for the robot cost function.



Disassembly time (t)

Figure 6: Condition 1: The robot cost function is either higher or lower than that of the human worker.



Disassembly time (t)

Figure 7: Condition 2: the robot cost function is lower than the human worker at the beginning and higher at the end.

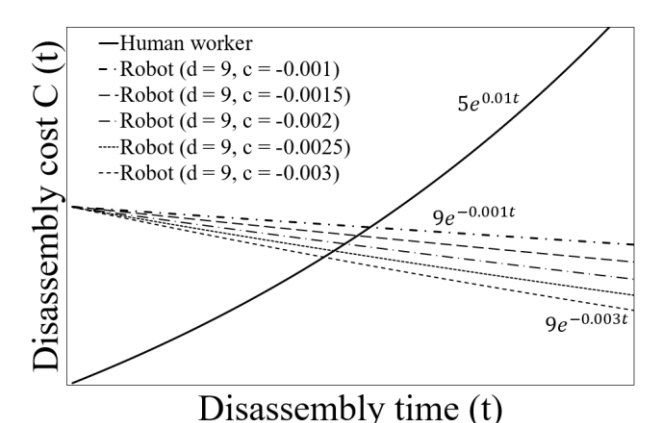


Figure 8: Condition 3: The cost function of the robot is higher than the human worker at the beginning and lower at the end.

In the first condition, the cost of the robot is either higher or lower than the human worker; in the second condition, the cost of the robot is lower than the human worker at the beginning but will be higher than human worker as the disassembly time increases; The third condition is the opposite of the second condition.

Table 8 summarizes the results of these three conditions for the work assignments between human and robot. In condition 1, when the parameters change slightly and the robot cost function is close to the human, the results are the same as in the previous section. However, the work assignments will change when the cost function deviates from humans. In condition 2, the work assignments are changed from the human worker to the robot as the parameter c increases. In condition 3, the work assignments are switched from robot to human as the parameter c decreases.

In reality, the cost function may vary from one case to another depending on the type of products, robots, and factory configurations. When estimating the operating cost of a robot, various factors should be considered, such as procurement cost, utilization rate, the efficiency of scheduling, tooling, and setup time. More accurate cost functions should incorporate these factors.

5. CONCLUSION

The study proposes a new optimization-based disassembly sequence planning framework for human-robot collaboration. It uses the multi-attribute theory to combine three attributes namely disassembly cost, disassembleability, and safety to determine the optimal disassembly sequence. The disassembly cost is modeled as an uncertain variable with a beta probability distribution. The safety and disassembleability are modeled using SI and DS scores. The model determines the task assignments among human and robot and determines the optimal disassembly sequence. An example of a desktop computer is used to show the application of the proposed model. In addition, a sensitivity analysis of the robot cost function is discussed.

Table 8: The work assignment results of the three sensitivity analysis conditions (R: robot; H: human worker).

Condition 1				Condition 2					Condition 3				
d = 3	d = 0.01	d = 7	d = 20	d = 1	d = 1	d = 1	d = 1	d = 1	d = 9	d = 9	d = 9	d = 9	d = 9
c =	c =	c =	c =	c =	c =	c =	c =	c =	c =	c =	c =	c =	c =
0.01	-0.000001	0.01	0.1	0.015	0.02	0.025	0.03	0.035	-0.001	-0.0015	-0.002	-0.0025	-0.003
R	R	R	R	R	R	R	R	R	R	R	Н	Н	Н
Η	Н	Н	R	Н	Н	R	R	R	Н	Н	Н	Н	Н
Η	Н	Н	R	Н	R	R	R	R	Н	Н	Н	Н	Н
R	R	R	R	R	R	R	R	R	R	R	R	R	R
Н	Н	Н	R	Н	Н	R	R	R	Н	Н	Н	Н	Н
Η	Н	Н	R	Н	Н	R	R	R	Н	Н	Н	Н	Н
R	R	R	R	R	R	R	R	R	R	R	R	R	Н
Η	Н	Н	R	Н	Н	Н	Н	R	Н	Н	Н	Н	Н
Н	Н	Н	R	Н	Н	Н	Н	R	Н	Н	Н	Н	Н
R	Н	R	R	R	R	R	R	R	Н	Н	Н	Н	Н
R	R	R	R	R	R	R	R	R	Н	Н	Н	Н	Н
Η	Н	Н	R	Н	R	R	R	R	Н	Н	Н	Н	Н
R	R	R	R	R	R	R	R	R	R	Н	Н	Н	Н
Η	Н	Н	R	Н	Н	R	R	R	Н	Н	Н	Н	Н
R	Н	R	R	R	R	R	R	R	Н	Н	Н	Н	Н
Н	Н	Н	R	Н	Н	Н	R	R	Н	Н	Н	Н	Н
Н	Н	Н	R	Н	Н	R	R	R	Н	Н	Н	Н	Н

This study can be extended in several ways. First, the SI scores and DS are currently decided subjectively using standard metrics and conducting lab experiments. However, computer vision techniques can be utilized to quantify the SI scores and DS by observing human and robot disassembly operations. Second, the model can be extended to a real-time sequence planner. Third, other attributes such as distance between the removal component and robotic arm position can be further considered in the real-time sequence planner. Fourth, experimental studies can be conducted to provide real disassemble time by robot and the feasibility analysis of each disassembly task.

ACKNOWLEDGEMENT

This material is based upon work supported by the National Science Foundation—USA under grant #2026276. Any opinions, findings, conclusions, or recommendations expressed in this material are those of the authors and do not necessarily reflect the views of the National Science Foundation.

REFERENCES

- [1] A. Khatun and N. Dhara, "E-Waste Management: A New Concern for Environmental Sustainability," in Smart Cities, Citizen Welfare, and the Implementation of Sustainable Development Goals, IGI Global, 2022, pp. 222–238.
- [2] Z. Wang, Q. Wang, B. Chen, and Y. Wang, "Evolutionary game analysis on behavioral strategies of multiple stakeholders in E-waste recycling industry," *Resour. Conserv. Recycl.*, vol. 155, p. 104618, 2020.

- [3] C. P. Garg, "Modeling the e-waste mitigation strategies using Grey-theory and DEMATEL framework," *J. Clean. Prod.*, vol. 281, p. 124035, 2021.
- [4] R. Zuidwijk and H. Krikke, "Strategic response to EEE returns:: Product eco-design or new recovery processes?," *Eur. J. Oper. Res.*, vol. 191, no. 3, pp. 1206–1222, 2008.
- [5] S. S. Smith and W.-H. Chen, "Rule-based recursive selective disassembly sequence planning for green design," *Adv. Eng. Informatics*, vol. 25, no. 1, pp. 77–87, Jan. 2011, doi: http://dx.doi.org/10.1016/j.aei.2010.03.002.
- [6] N. Nasr and M. Thurston, "Remanufacturing: A key enabler to sustainable product systems," *Rochester Inst. Technol.*, p. 23, 2006.
- [7] S. Behdad and D. Thurston, "Disassembly and Reassembly Sequence Planning Tradeoffs Under Uncertainty for Product Maintenance," *J. Mech. Des.*, vol. 134, no. 4, p. 041011, 2012, doi: 10.1115/1.4006262.
- [8] B. Yu, E. Wu, C. Chen, Y. Yang, B. Z. Yao, and Q. Lin, "A general approach to optimize disassembly sequence planning based on disassembly network: A case study from automotive industry," *Adv. Prod. Eng. Manag.*, vol. 12, no. 4, pp. 305–320, 2017.
- [9] M. V. A. R. Bahubalendruni and V. P. Varupala, "Disassembly sequence planning for safe disposal of end-of-life waste electric and electronic equipment,"

- Natl. Acad. Sci. Lett., vol. 44, no. 3, pp. 243–247, 2021.
- [10] H.-E. Tseng, Y.-M. Huang, C.-C. Chang, and S.-C. Lee, "Disassembly sequence planning using a Flatworm algorithm," *J. Manuf. Syst.*, vol. 57, pp. 416–428, 2020, doi: https://doi.org/10.1016/j.jmsy.2020.10.014.
- [11] Y. Fu, M. Zhou, X. Guo, L. Qi, and K. Sedraoui, "Multiverse Optimization Algorithm for Stochastic Biobjective Disassembly Sequence Planning Subject to Operation Failures," *IEEE Trans. Syst. Man, Cybern. Syst.*, 2021.
- [12] X. Xia, H. Zhu, Z. Zhang, X. Liu, L. Wang, and J. Cao, "3D-based multi-objective cooperative disassembly sequence planning method for remanufacturing," *Int. J. Adv. Manuf. Technol.*, vol. 106, no. 9, pp. 4611–4622, 2020, doi: 10.1007/s00170-020-04954-2.
- [13] S.-C. Lee, H.-E. Tseng, C.-C. Chang, and Y.-M. Huang, "Applying Interactive Genetic Algorithms to Disassembly Sequence Planning," *Int. J. Precis. Eng. Manuf.*, vol. 21, no. 4, pp. 663–679, 2020, doi: 10.1007/s12541-019-00276-w.
- [14] S. Behdad and D. Thurston, "Disassembly process planning tradeoffs for product maintenance," in *International Design Engineering Technical Conferences and Computers and Information in Engineering Conference*, 2010, vol. 44144, pp. 427–434.
- [15] K. Li, Q. Liu, W. Xu, J. Liu, Z. Zhou, and H. Feng, "Sequence planning considering human fatigue for human-robot collaboration in disassembly," *Procedia CIRP*, vol. 83, pp. 95–104, 2019.
- [16] S. Vongbunyong, S. Kara, and M. Pagnucco, "Basic behaviour control of the vision-based cognitive robotic disassembly automation," *Assem. Autom.*, 2013.
- [17] W. Xu, Q. Tang, J. Liu, Z. Liu, Z. Zhou, and D. T. Pham, "Disassembly sequence planning using discrete Bees algorithm for human-robot collaboration in remanufacturing," *Robot. Comput. Integr. Manuf.*, vol. 62, p. 101860, 2020, doi: https://doi.org/10.1016/j.rcim.2019.101860.
- [18] M.-L. Lee, S. Behdad, X. Liang, and M. Zheng, "A Real-Time Receding Horizon Sequence Planner for Disassembly in a Human-Robot Collaboration Setting," in 2020 International Symposium on Flexible Automation, 2020.
- [19] S. Parsa and M. Saadat, "Human-robot collaboration disassembly planning for end-of-life product disassembly process," *Robot. Comput. Integr. Manuf.*, vol. 71, p. 102170, 2021.
- [20] C. Xu, H. Wei, X. Guo, S. Liu, L. Qi, and Z. Zhao,

- "Human-Robot Collaboration Multi-objective Disassembly Line Balancing Subject to Task Failure via Multi-objective Artificial Bee Colony Algorithm," *IFAC-PapersOnLine*, vol. 53, no. 5, pp. 1–6, 2020.
- [21] W. Xu, J. Cui, B. Liu, J. Liu, B. Yao, and Z. Zhou, "Human-robot collaborative disassembly line balancing considering the safe strategy in remanufacturing," *J. Clean. Prod.*, vol. 324, p. 129158, 2021.
- [22] J. Fischer, P. Stock, and G. Zülch, "Simulation of Disassembly and Re-assembly Processes with Beta-distributed operation Times," in *Integrating Human Aspects in Production Management*, Springer, 2005, pp. 147–156.
- [23] S. Parsa and M. Saadat, "Intelligent selective disassembly planning based on disassemblability characteristics of product components," *Int. J. Adv. Manuf. Technol.*, vol. 104, no. 5, pp. 1769–1783, 2019, doi: 10.1007/s00170-019-03857-1.
- [24] J. Steven Moore and A. Garg, "The strain index: a proposed method to analyze jobs for risk of distal upper extremity disorders," *Am. Ind. Hyg. Assoc. J.*, vol. 56, no. 5, pp. 443–458, 1995.
- [25] D. L. Thurston, "Utility function fundamentals," *Decis. Mak. Eng. Des.*, pp. 15–19, 2006.
- [26] D. L. Thurston, K. Lewis, W. Chen, and L. C. Schmidt, "Multi-attribute utility analysis of conflicting preferences," *Decis. Mak. Eng. Des.*, pp. 125–133, 2006.
- [27] D. L. Thurston, J. V Carnahan, and T. Liu, "Optimization of Design Utility," *J. Mech. Des.*, vol. 116, no. 3, pp. 801–808, Sep. 1994, doi: 10.1115/1.2919453.
- [28] R. T. Clemen and T. Reilly, *Making hard decisions* with *DecisionTools*. Cengage Learning, 2013.
- [29] C. H. Glock, E. H. Grosse, T. Kim, W. P. Neumann, and A. Sobhani, "An integrated cost and worker fatigue evaluation model of a packaging process," *Int. J. Prod. Econ.*, vol. 207, pp. 107–124, 2019.
- [30] V. Potkonjak, V. Petrović, K. Jovanović, and D. Kostić, "Human-Robot Analogy—How Physiology Shapes Human and Robot Motion," in *ECAL 2013: The Twelfth European Conference on Artificial Life*, 2013, pp. 136–143.
- [31] M. Pearce, B. Mutlu, J. Shah, and R. Radwin, "Optimizing makespan and ergonomics in integrating collaborative robots into manufacturing processes," *IEEE Trans. Autom. Sci. Eng.*, vol. 15, no. 4, pp. 1772–1784, 2018.